Origin of Strong Excitation Wavelength Dependent Fluorescence of Graphene Oxide

Scott K. Cushing,[†,‡,#] Ming Li,[†,#] Fuqiang Huang,[§] and Nianqiang Wu[†,*]

[†]Department of Mechanical and Aerospace Engineering, West Virginia University, Morgantown, West Virginia 26506-6106, United States, [‡]Department of Physics, West Virginia University, Morgantown, West Virginia 26506-6315, United States, and [§]Shanghai Institute of Ceramics, Chinese Academy of Sciences, Shanghai 200050, People's Republic of China. [#]S. K. Cushing and M. Li contributed equally to this work.

ABSTRACT The peak fluorescence emission of conventional fluorophores such as organic dyes and inorganic quantum dots is independent of the excitation wavelength. In contrast, the position of the peak fluorescence of graphene oxide (GO) in a polar solvent is heavily dependent on the excitation wavelength. The present work has discovered that the strong excitation wavelength dependent fluorescence in GO is originated from the "giant red-edge effect", which breaks Kasha's rule. When GO sheets are present in a polar solvent, the solvation dynamics slow down to the same time scale as the fluorescence due to the local environment of the GO sheet. Consequently, the fluorescence peak of GO broadens and red-shifts up to 200 nm with an increase in the excitation wavelength. The giant red-edge effect of GO disappears in a nonpolar solvent, leading to a narrow fluorescence peak that is independent of the excitation wavelength. Discovery of the underlying strong excitation wavelength dependent fluorescence mechanism provides guidelines for the design of graphene oxide-based optical devices.

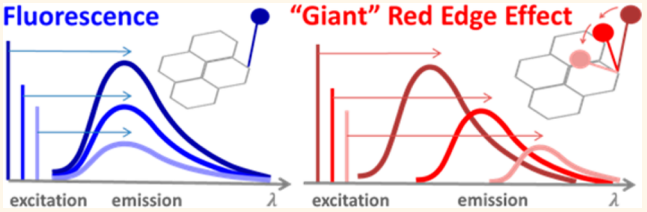

KEYWORDS: graphene · graphene oxide · giant red-edge effect · fluorescence · photoluminescence · excitation wavelength dependent luminescence

The discovery of the remarkable electronic and structural properties of graphene has revolutionized the scientific community.[1−4] The linear band structure of graphene leads to its applications in single-electron transistors and flexible electronics. However, the zero optical band gap of the Dirac cone in graphene prevents it from being luminescent. To enable photoluminescence, the band gap of graphene is opened by reducing its size to the nanometer scale[5−9] and introducing defects[10−12] or by modifying its two-dimensional (2D) carbon−carbon network with functional groups.[13,14] One of the functionalized forms is graphene oxide (GO), which consists of various oxygen-containing groups, resulting in a broad-band fluorescence. A recent report shows that the fluorescence peaks are originated from the electronic transitions at different energy levels.[15] The fluorescence of GO and GO nanodots is characterized by several new, exotic phenomena, expanding graphene's remarkable properties to the realm of luminescence. The luminescence of GO is very broad and spans from the ultraviolet (UV) to the near-infrared (NIR) range. The broad luminescence can be tuned by pH, reduction level, and size across a range similar to that of quantum dots, but with the added advantages of low cost, nontoxicity, and chemical stability.[12−26] However, the most intriguing luminescent property of GO is that its fluorescence peak position can be tuned by simply varying the excitation wavelength without changing its chemical composition and size.

In general, the peak photoluminescence of conventional fluorophores, such as organic dyes and inorganic quantum dots, is independent of the wavelength of the excitation source because the excited electrons relax to the band edge before fluorescence begins regardless of their initial excitation energy.[27] The peak fluorescence wavelength of organic dyes and quantum dots is the same as long as the electrons are excited within the same band. Small

* Address correspondence to nick.wu@mail.wvu.edu.

Received for review November 11, 2013 and accepted December 21, 2013.

Published online December 21, 2013
10.1021/nn405843d

© 2013 American Chemical Society

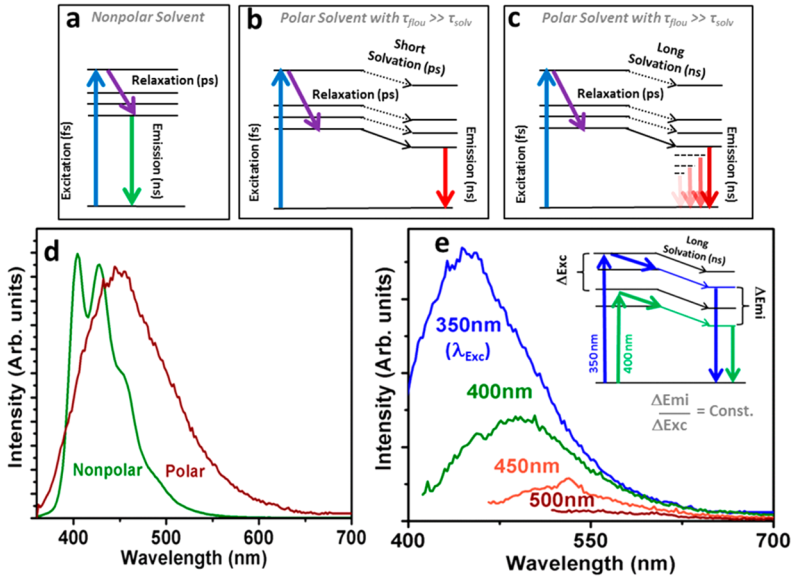

Figure 1. Wavelength-dependent fluorescence from solvent environment. (a) Fluorescence in a nonpolar solvent proceeds through excitation (fs), thermal relaxation of carriers (ps), and emission (ns). (b) In a polar solvent, solvent relaxation acts to lower the energy of the excited state and red-shift the emission. However, the solvation duration is much shorter than fluorescence lifetime. (c) If the solvent interactions are on the same time scale as the fluorescence lifetime, a time-dependent emission is created, resulting in a red-edge tail. (d) The fluorescence of GO in a nonpolar solvent (pentane) is independent of excitation wavelength. In a polar solvent (water) the solvation process red-shifts the emission energy and broadens the spectrum. (e) The relaxation of the time-dependent emission energy is independent of excitation wavelength, so shifting the excitation wavelength shifts the emission wavelength proportionally, creating an excitation wavelength dependent fluorescence as seen in GO in water. The excitation wavelength is labeled for each emission curve.

excitation wavelength dependent shifts, however, have been reported in highly rigid environments such as glasses, viscous polymers, proteins, and membranes.[28−33] In contrast, the fluorescence peak of GO exhibits a large red-shift with an increase in the excitation wavelength without the need of low temperatures or viscous solvents.[12−26] For example, the difference between the emission peak and the excitation wavelength shows a red-shift of ∼220 nm from the visible to NIR in water at room temperature as the excitation energy changes from the UV to the visible range.[15] Despite the excellent studies of several groups,[16,18,34,35] the mechanism of strong excitation wavelength dependent fluorescence of GO remains a mystery, preventing the development of novel technologies based on this very intriguing property.

In the present work GO sheets, chemically reduced GO sheets rich in the −OH moiety, and oxidized GO sheets rich in the −COOH moiety have been prepared to unravel the underlying mechanism of strong excitation wavelength dependent fluorescence. Time-resolved fluorescence is measured for each of the GO samples in solvents with different polarities. Our experimental results and theoretical analysis show that the spectral shape of the fluorescence of GO can be explained as the collection of an excited-state protonation from the −COOH group and an excitation wavelength dependent fluorescence from the polar groups such as the −OH moiety in the GO sheets. The −COOH groups lead to a pH-dependent emission through an excited-state protonation.[16,18] When GO is in a polar solvent and excited by a light source, a slow solvent relaxation process occurs on the same time scale as the fluorescence emission, inducing a "giant red-edge effect". The slow solvent relaxation is caused by the local environment of the GO sheets. The giant red-edge effect is unprecedentedly discovered to be the origin of the strong excitation wavelength dependent fluorescence of GO.

RESULTS AND DISCUSSION

Wavelength-Dependent Fluorescence. Classically, the position of the fluorescence peak is independent of the wavelength of the excitation source because of the time scale of the processes involved. Fluorescence in a noninteracting environment (gas or nonpolar solvent) is depicted in Figure 1a and proceeds through the absorption of light (10^{-15} s), nonradiative relaxation to the band edge (10^{-12} s), and radiative recombination of the electron and hole to emit a photon (10^{-9} s).[27] The fluorescence does not depend on excitation energy because all excited electrons, independent of initial energy, have relaxed to the band edge before fluorescence proceeds. The limit of band edge emission is called Kasha's rule.[36] For example, the fluorescence of GO in pentane (a nonpolar solvent) exhibited a relatively narrow bandwidth, as experimentally demonstrated in Figure 1d.

In an interacting environment, such as a polar solvent, an additional relaxation step (solvation) occurs

in the fluorescence process. After excitation, the fluorophore and the solvent dipole are no longer in equilibrium. The solvent dipole can rotate to align with the excited fluorophore, reducing the interaction energy and lowering the energy of the excited fluorophore (Figure 1b). The relaxation time of common polar organics solvents is ~10 ps, while the fluorescence lifetime of organic dyes is several nanoseconds.[37] Therefore, the solvation process is usually complete before fluorescence emission, and the net result of solvent relaxation is to red-shift the fluorescence (Figure 1b). The red-shift is referred to as a solvatochromic shift.[27] This trend was confirmed by comparing the fluorescence of GO in a nonpolar solvent (such as pentane) and a polar solvent (such as water), as shown in Figure 1d. The fluorescence of GO was broadened and red-shifted in the polar solvent due to the solvent interactions.

If the solvation dynamics is not an order of magnitude quicker than the fluorescence lifetime, the fluorophore can emit simultaneously to the excited state's energy being reduced, creating a time-dependent emission energy (Figure 1c). This phenomenon is called the "red-edge effect",[33,38−40] which makes the fluorescence peak dependent on the excitation wavelength. For example, the emission peak of GO in water, determined by the center of gravity of the fluorescence, was at 440 nm under excitation at 350 nm, but red-shifted to 580 nm under excitation at 500 nm (Figure 1e). The rate of change in the time-dependent emission energy due to solvation is the same regardless of the excitation wavelength, as long as the final solvated energy is not reached in the fluorescence lifetime.[27] Therefore, different excitation wavelengths undergo the same relaxation process and emit with the same spectral form, only offset by the initial difference in excitation wavelength (Figure 1e). That is, the slope of the change in the peak emission wavelength for a given change in excitation wavelength, $\Delta\lambda_{emission}/\Delta\lambda_{excitation}$, remains a constant throughout most of the excitation spectrum, creating a linear slope of $\Delta\lambda_{emission}/\Delta\lambda_{excitation}$ up to ~460 nm, as seen in Figure S1. For further red-shifted excitation wavelengths, the final solvated energy can be approached in the fluorescence lifetime, and no more shift of the peak emission is possible. The matching of the complete solvation lifetime to the fluorescence lifetime therefore leads to an exponential limit of the ratio of $\Delta\lambda_{emission}/\Delta\lambda_{excitation}$ as the excitation wavelength approaches the final solvated energy (Figure S1).

The behavior of excitation wavelength dependent fluorescence is therefore strongly affected by the time scale of the solvation step (Figure 1c). One route to shorten the solvent relaxation time is to increase the temperature. To show the effect of the solvation lifetime on the red-edge effect, the fluorescence of GO in water was tested at different temperatures. When the temperature increases, the solvation can complete before fluorescence begins. Consequently, the red-edge effect began to disappear at 80 °C, as shown in Figure S1. The final solvated energy is also seen to blue-shift with increasing the temperature because the solvation process is complete before the fluorescence lifetime.

It has been reported that the fluorescence of GO and GO nanodots is associated with the aromatic C═C, the C−OH, and the COOH (or C═O) functional groups that commonly exist on the GO sheets.[15] It is believed that the contributions to fluorescence can be separated into two main branches: (i) a pH-dependent component associated with the protonating groups (carboxyl) and (ii) a non-pH-dependent emission present after reduction reactions (epoxide and hydroxyl).[10,16,18,41,42] pK_a* values have shown that the −COOH group is responsible for the pH-dependent emission, while selective reduction procedures have confirmed that the hydroxyl group is primarily responsible for the non-pH-dependent emission.[10,16,18,41,42]

To effectively separate and further explore the origins of the pH-dependent and the excitation wavelength dependent fluorescence, the GO was chemically treated in HNO_3 and KOH solutions to create −COOH-rich and −OH-rich GO, respectively.[15] The characterization details are seen in Figure S2. The UV−visible absorption spectrum of GO is shown in Figure 2h. The molecule-like absorption in GO was assigned to the $\pi\rightarrow\pi^*$ transitions at 230 nm and to the $n\rightarrow\pi^*$ transition at 305 nm, consistent with literature.[10,15,16,18] In addition to the localized electron density, the underlying band structure of the graphene sheet still existed, as confirmed by an absorption tail that decays exponentially to a constant value in the NIR.[43] The band structure is not identical to that of pure graphene, but is similar to that of graphene sheets where a band gap has been opened through defects and doping.[44]

After chemical treatment, the local molecular structure became dominated either by the −OH or by the −COOH groups. After treatment in KOH solution, the $n\rightarrow\pi^*$ transition strength was reduced, and the $\pi\rightarrow\pi^*$ peak red-shifted to 250 nm due to the increased number of electron-donating groups (Figure 2b).[27] The −COOH-rich GO blue-shifted the $\pi\rightarrow\pi^*$ transition to 200 nm and increased the $n\rightarrow\pi^*$ transition strength (Figure 2e). The NIR tail was constant, which was independent of chemical treatment. It is worth noting that the UV−visible absorption of GO was a combination of the optical transitions from both the −OH-rich and the −COOH-rich GO, which confirmed that the optical properties were originated from these functional groups.

The UV−visible absorption measurements indicate the optical properties of GO are explicitly determined by which functional groups are present to donate local

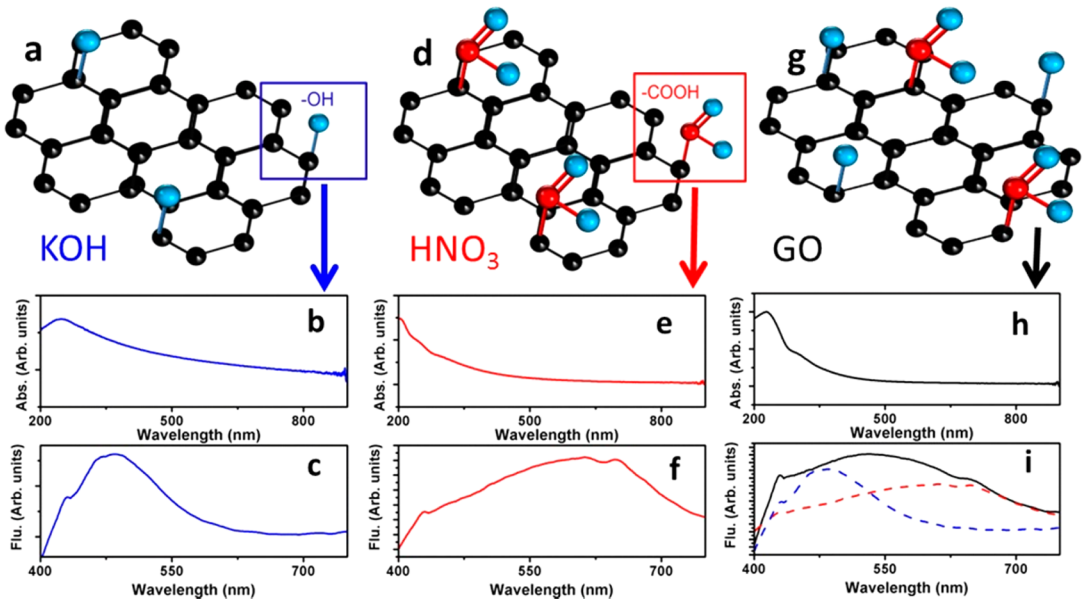

Figure 2. Optical properties of functionalized graphene oxide (GO). (a) The −OH-rich GO and (d) the −COOH-rich GO and (g) GO; the UV−visible absorption spectra of (b) the −OH-rich GO and (e) the −COOH-rich GO and (h) GO; the fluorescence spectra of (c) the −OH-rich GO and (f) the −COOH-rich GO and (i) GO. The pH of the −OH rich, −COOH rich, and pristine GO was 7, 3, and 5, respectively. The fluorescence was measured in water with the concentration adjusted to keep the absorption below 0.1 OD to avoid inner filter effects.

electron density and allow optical transitions. The fluorescence also reflects this trend. The fluorescence of the −OH-rich GO with an excitation wavelength of 350 nm is shown in Figure 2c. The −OH-rich GO had an emission peak centered at ∼500 nm, which was originated from the electronic transitions ($\pi^*\rightarrow$n and $\pi^*\rightarrow\pi$). The molecular nature of the fluorescence in the −OH-rich GO was further confirmed by the fluorescence spectrum obtained in a nonpolar solvent (Figure S3). In the absence of solvent interactions, the fluorescence was observed to be a mirror image of the excitation spectrum (Figure S3).

The −COOH-rich GO in Figure 2f showed a very different fluorescence spectrum compared to the −OH-rich GO despite their only being small changes in the UV−visible absorption between the two functional groups. The −COOH-rich GO had a broad emission band centered at ∼630 nm with a half-width of ∼250 nm. The emission was not representative of a simple molecular transition. Previous reports have shown that a broadband emission is present identical to the COOH-rich GO at low pH, while an emission identical to the −OH-rich GO is present at a range from neutral to high pH.[16,18] The pH-dependent fluorescence shown in these studies indicates that the −COOH group was undergoing an excited-state protonation. Here, our results, which show pH-dependent emission for the −COOH and not −OH-rich GO, confirm the pK_a* value-based hypothesis that the COO^- group undergoes an excited-state protonation, creating a broad emission at low pH.

The fluorescence of GO is shown in Figure 2i. Similar to the UV−visible absorption, the fluorescence of the GO was observed to be well represented by a superposition of the fluorescence of both the −COOH-rich and the −OH-rich GO sheets. Therefore, the complete fluorescence mechanism of GO can be described as shown in Figure 3. The fluorescence is composed of an excited-state protonation of the −COOH group and an excitation wavelength dependent fluorescence from the polar groups such as the −OH moiety in the GO sheets. The two components combine to create the broad fluorescence emission of GO at low pH (the inset in Figure 3). At high pH or after chemical reduction of GO in the KOH solution, the polar groups such as the −OH moiety dominate the fluorescence emission with an excitation wavelength dependent behavior. The excitation wavelength dependence of fluorescence occurs because of the relaxation between the solvent dipole and the excited state of GO. After excitation, the excited GO dipole is not aligned with the solvent. As the solvent rotates, the emission energy decreases for the GO. The GO fluoresces on the same time scale as the solvent relaxation, creating a time-dependent energy, as shown on the left side of Figure 3.

Dynamics of Solvent Relaxation. As mentioned above (Figure 1c), the phenomenon of excitation wavelength dependent fluorescence is due to the presence of a slowed solvation process during fluorescence emission. Therefore, time-resolved fluorescence (TRF) measurements were used to investigate the origin of giant red-edge effect in GO. A simple model for solvent relaxation must first be established to interpret the TRF results. Solvent relaxation can be described theoretically by the time-dependent emission energy[27,45−47]

$$\hbar\omega_{em}'(t) = \hbar\omega_{exc}(0) - \hbar\omega_{solv}(t) \quad (1)$$

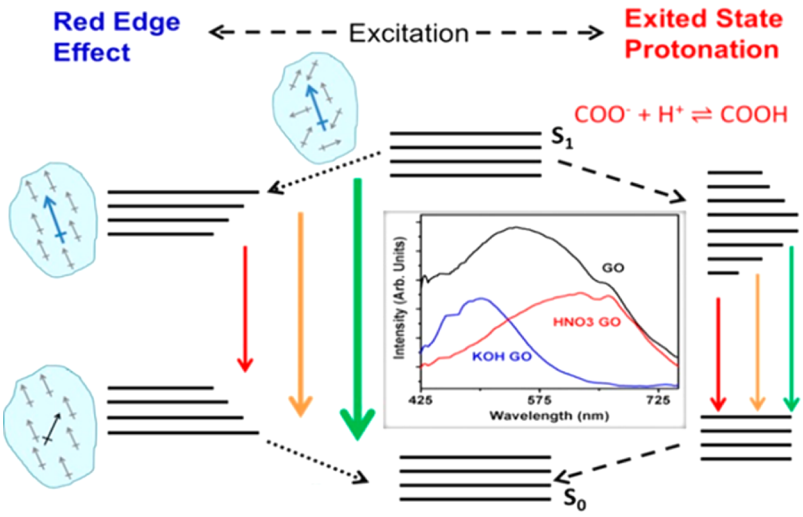

Figure 3. Fluorescence mechanism of graphene oxide (GO). The fluorescence of GO (inset middle) is composed of an excited-state protonation from the −COOH group (on the right side) and the excitation wavelength dependent fluorescence from the polar groups such as the −OH moiety in the GO sheets (on the left side). The fluorescence shown was measured in water at pH 7 and 3 for the −OH-rich and −COOH-rich GO.

which can be rewritten as

$$U_{em}'(t) = U_{exc}(0) - U_{solv}(t) \quad (2)$$

The time-dependent emission energy, $U_{em}'(t)$, represents the lowering of the excited state's energy with time as the solvent rotates (Figure 4a). $U_{exc}(0)$ is the fluorescence at $t = 0$ immediately after excitation. If the red-edge effect is absent, $U_{em}'(t) = U_{exc}(0)$ and the fluorescence emission process is identical to that in a nonpolar solvent. $U_{solv}(t)$ describes the interaction energy of the solvent dipole and fluorophore as they align and is given by[27,45−47]

$$U_{solv}(t) = \vec{\mu}_{fluo} \cdot \vec{R}(t) \quad (3)$$

where $R(t)$ is the reaction field, which incorporates the electrodynamics response of the solvent to the change in the fluorophore when excited. $U_{solv}(t)$ is a function of the solvent dipole, fluorophore dipole, and interaction energy:

$$U_{solv}(t) = U_{solv}(\mu_{fluo}, \mu_{solv}, \Theta(t)) \quad (4)$$

where $\Theta(t)$ represents the rotation of the solvent dipole to minimize the interaction energy (Figure 4a). A simple Brownian rotator model $\Theta(t)$ can be represented as[45]

$$\Theta(t) = \Theta_0 e^{-t/\tau_{solv}} \quad (5)$$

In most organic solvents, the fluorescence lifetime (τ_{fluo}) is much longer than the solvent relaxation time (τ_{solv}), or $\tau_{fluo} \gg \tau_{solv}$. This means that the effect of solvation is only to red-shift the fluorescence by a fixed amount as discussed in Figure 1b, or

$$U_{em}'(\tau_{fluo}) = U_{exc}(0) - U_{solv}(\infty) \quad (6)$$

No time-dependent terms exist in the fluorescence energy in this case. The red-shift is determined only by the polarity of the solvent, expressed by the well-known solvatochromic shift formula between the absorbance peak and fluorescence peak (cm^{-1}) as[27]

$$\bar{\nu}_{abs} - \bar{\nu}_{fluo} = \frac{U_{em}'(\tau_{fluo})}{hc} - \frac{U_{exc}(0)}{hc} = \frac{U_{solv}(\infty)}{hc} = \frac{2(\Delta\mu)^2}{hca^3}\left[\left(\frac{\varepsilon - 1}{2\varepsilon + 1}\right) + \left(\frac{n^2 - 1}{2n^2 + 1}\right)\right] \quad (7)$$

where $\Delta\mu$ is the change in the dipole moment of the fluorophore upon excitation in Debyes, a is the Onsager cavity radius (Å), ε is the dielectric constant, h is Planck's constant (ergs), c is the speed of light (cm/s), and n is the refractive index.[27]

If $\tau_{fluo} \cong \tau_{solv}$, then the time dependence of the excited state's energy must be taken into account by

$$U_{em}'(t) = U_{exc}(0) - U_{solv}(t) \quad (8)$$

The change in fluorescence emission energy with time, $U_{em}'(t)$, can be measured experimentally by collecting the TRF at several emission wavelengths for one excitation wavelength (Figure 4c). In GO, fluorescence excited with a 460 nm pulse is immediately detected at 500 nm at $t = 0$ (Figure 4c). The TRF trace for 500 nm emission represents the fluorescence before solvation begins, or $U_{em}'(t) = U_{exc}(0)$, and is centered at $t = 0$. According to a global fit, the fluorescence at 500 nm decays triexponentially in time after the initial excitation with average time constants of 190 ps, 1.5 ns, and 5.8 ns. These time constants are similar to those obtained under 370 nm excitation (Figure S4).

The TRF trace for fluorescence at 520 nm looks identical to 500 nm (Figure 4c), except that it is no

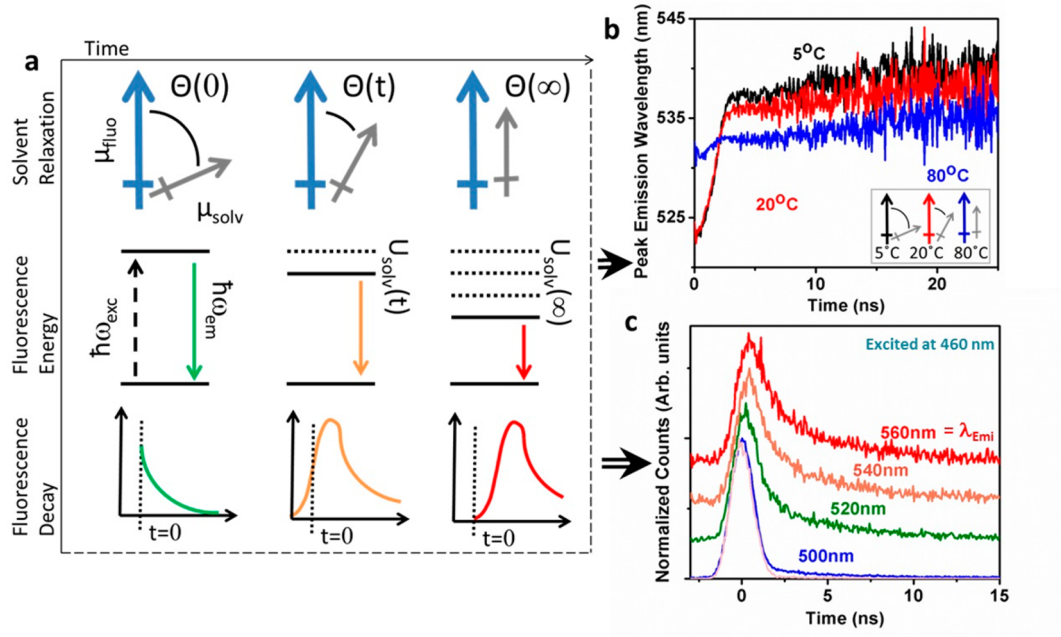

Figure 4. Effect of solvent relaxation on time-resolved fluorescence. (a) The solvent dipole aligns with the excited GO fluorophore to minimize the interaction energy. (b) The fluorescence emission maximum after 460 nm excitation decreases until the solvent is fully relaxed, creating the time-dependent fluorescence spectra. (c) The peak intensity of the time-resolved emission spectra (TRES) increases in wavelength after initial excitation at 460 nm but decays uniformly, mapping out the solvent relaxation in time. The instrument response is shown by the pink line. The fluorescence was measured in water at pH 7 with the concentration adjusted to keep the absorption below 0.1.

longer centered at $t = 0$. Rather, it is centered at some later time t'. This is a direct result of $U_{em}'(t)$ depending on time, or the band energy lowering as represented in Figure 1c. If τ_{fluo} was much larger than τ_{solv}, the fluorescence would be centered at $t = 0$ for all emission wavelengths since all excited electrons would have relaxed to the band edge by the time fluorescence begins (Figure 1b). This is not the case for GO; the band edge energy is now lowering as fluorescence proceeds, and the TRF peaks at later times for red-shifted emission wavelengths. Figure 4c reflects the changes in $U_{em}'(t)$ for GO. That is, as the 500 nm emission decays, the TRF peaks at 520 nm, 540 nm, and then 560 nm. The triexponential relaxation dynamics does not depend on the measured emission wavelength. It should be emphasized that the peak emission is determined by the center of mass of the fluorescence. The peak spectral form is not changing; the center wavelength is just being shifted to higher wavelengths.

The frequency of the emission maximum can be plotted *versus* time as shown in Figure 4b to directly measure $U_{em}'(t)$. The plot of $U_{em}'(t)$ can then be fit to extract the solvation lifetime using a normalized correlation function and assuming that $\Theta(t)$ follows Brownian dynamics (eq 5). The correlation function in this approximation is defined as[38,45]

$$c(t) = \frac{U_{em}'(\infty) - U_{em}'(t)}{U_{em}'(\infty) - U_{em}'(0)} = \frac{\lambda_\infty - \lambda}{\lambda_\infty - \lambda_0} = e^{-t/\tau_{solv}} \quad (9)$$

The simple Brownian rotator model fails to completely capture the decay dynamics, but is a good approximation.[33,38−40] The correlation function, or $U_{em}'(t)$, decays with a time of $\tau_{solv} = 650$ ps. This time constant is similar to the main component of the triexponential decay of the OH-rich GO after treatment in KOH solution, $\tau_{fluo} = 650$ ps (Figure S4), which has confirmed that this functional group is related to the excitation wavelength dependent dynamics. The excited-state protonation is reflected as a slight decay of the long time scale maximum in the correlation plots.

Red-Edge Effect Induced by Solvation Dynamics. The TRF measurements confirmed that the fluorescence lifetime, $\tau_{fluo} = 650$ ps, is equal to the solvation lifetime, $\tau_{solv} = 650$ ps, and the necessary conditions therefore exist to allow the red-edge effect. However, the time-dependent solvation dynamics of Figure 4 must be linked to the excitation wavelength dependence of the steady-state fluorescence of Figure 1. The static fluorescence is the long time scale average of the time-dependent dynamics. Mathematically, this is represented as the steady-state fluorescence being the time integral of the full time and frequency-dependent TRF, or time-resolved emission spectrum (TRES), shown in Figure S5,[27]

$$F(\omega) = \int_0^\infty f(\omega, t)\, dt \quad (10)$$

where the TRES is represented by[27]

$$f(\omega, t) = g(\omega - \omega(t))e^{-t/\tau_{fluo}} \quad (11)$$

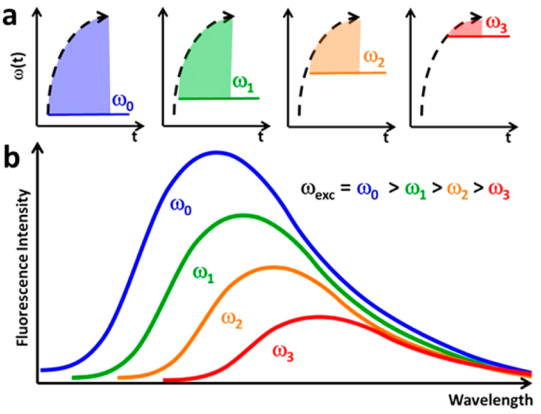

Figure 5. Solvation dynamics and the red-edge effect. The time-resolved dynamics is related to the steady-state fluorescence by the time integral of the time dependent emission energy $\omega(t)$ created by alignment of the solvent dipole with the excited fluorophore. Shifting the excitation frequency (a) from ω_0 to ω_1 is equivalent to changing the starting time of the integration from $\omega(t)$ to $\omega(t')$. As the excitation frequency is red-shifted, the same steady-state fluorescence spectrum is produced (b), but shifted in peak position and lowered in intensity proportional to the area under $\omega(t')$. The shift of the peak position will be functionally similar to $\omega(t)$, predicting the slope of the emission wavelength with changing excitation wavelength.

under the assumption of only a single exponential decay and that $g(\omega - \omega(t))$ is a Gaussian or log-normal distribution representing the spectral shape of the TRF plots.[27] The function $g(\omega - \omega(t))$ represents a vertical cut in time for Figure S5, while the exponential decay represents a horizontal cut in frequency. $F(\omega)$ is what is measured experimentally in a steady-state spectrofluorometer, while $f(\omega,t)$ is what is measured at each wavelength in TRF. The sum of the photons detected in TRF gives the intensity of the fluorescence at that frequency in the steady-state measurement.

In the function $g(\omega - \omega(t))$, $\omega(t)$ is directly related to the correlation function $c(t)$ (eq 9) and describes the shift in the TRF peak offset with wavelength in Figure 4b and c. If the solvent is nonpolar, then $\omega(t)$ equals zero and the integral of eq 11 gives the static fluorescence spectrum. If the solvent is polar and $\tau_{fluo} \gg \tau_{solv}$, then $\omega(t)$ equals $\omega(\infty)$ and the integral of eq 11 gives the fluorescence spectrum shifted according to the solvatochromic shift formula, eq 5. If the solvent is polar and $\tau_{fluo} \cong \tau_{solv}$, the time dependence of $\omega(t)$ weights the spectral integral toward longer wavelengths, creating a red-shifted emission tail (hence red-edge effect) as reflected in Figure 1e.

The importance of $\omega(t)$ is not just in creating a red-shifted emission tail. $\omega(t)$ is the link between the solvation dynamics and the excitation-dependent fluorescence, as represented schematically in Figure 5. Let the initial excitation energy be ω_0. After excitation at energy $\omega(t = 0) = \omega_0$, the peak intensity of the TRF shifts by $\omega(t)$. This change is represented by the curved arrow in Figure 5a, which is simply a map of the central peak in the full 2D TRES spectrum. The time integral of $\omega(t)$ is represented by the shaded area and gives the steady-state fluorescence by eq 10, represented by the blue curve in Figure 5b. Now, if the excitation energy is decreased so that ω_1 is less than ω_0, the change in frequency $\Delta\omega$ is equal to ω_0 minus ω_1, and this is equivalent to making

$$\omega(t = 0) = \omega_0 - \Delta\omega = \omega(t') \tag{12}$$

or starting the integration of eq 10 at some delayed time t' (panel 2 in Figure 5a). As long as the time is in the linear range of the correlation function, the integral of eq 10 does not change for a shift in time to t' since

$$\begin{aligned} g(\omega - \omega(t')) &= g(\omega - (\omega(t) - \Delta\omega)) \\ &= g(\omega' + \omega(t)) \end{aligned} \tag{13}$$

This gives

$$F(\omega) = \int_{t'}^{\infty} f(\omega, t)\, dt = \int_{0}^{\infty} f(\omega', t)\, dt = F(\omega') \tag{14}$$

which is unchanged for a shift in excitation ω'. This means the integral of eq 10 will give the same spectral form for ω_1 as ω_0, but reduced in intensity by the change in area under $\omega(t')$ and shifted to a lower energy by $\Delta\omega$. Thus the ratio of $\Delta\lambda_{emission}/\Delta\lambda_{excitation} \cong 1$ and a linear slope exists for the giant red-edge effect in GO for $\omega_{exc} < \omega(\infty)$ (Figure S1).

As the excitation energy approaches $\omega(\infty)$, the area under the curve of $\omega(t)$ decreases according to the measured correlation function (Figure 4b), so the slope of the $\Delta\lambda_{emission}/\Delta\lambda_{excitation}$ shift goes asymptotically to a constant value in an exponential fashion (Figure S1) for the assumption of a Brownian rotator model. It must be remembered that fluorescence can be excited with increasing wavelength only if the density of states exists in the ground state. The UV−visible absorbance of GO has an exponential tail (Figure S6) due to the coupling of the local electron density of the surface groups with the underlying band structure of the graphene sheet, allowing for the excitation of fluorescence well to $\omega(\infty)$ and the giant red-edge effect to be measured.

The extent of the red-edge effect will depend on temperature since $\omega(t)$, which is itself modeled by a temperature-dependent Brownian rotator (eq 5), determines the extent of the red-edge effect. The solvent dipole rotation is therefore a function of its thermal energy:[27]

$$\tau_{solv} = \frac{\eta V}{k_b T} \tag{15}$$

where η is the viscosity, V is the volume, and k_b is the Boltzmann constant. The solvent rotation τ_{solv} is slower at 5 °C, allowing the emission from a lower energy state than 20 and 80 °C (Figure S1) since $\omega(t)$ takes longer to approach $\omega(\infty)$. When the temperature increased to 80 °C, then $\tau_{fluo} \gg \tau_{solv}$ and the red-edge effect was

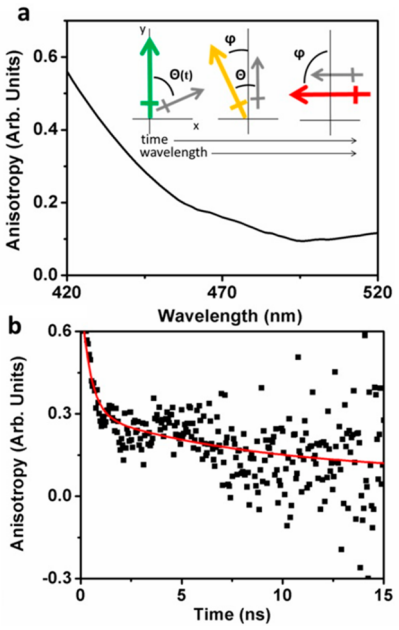

Figure 6. Anisotropy for GO fluorescence. (a) The steady-state anisotropy under 400 nm excitation decreases as the wavelength increases due to the relaxation of the solvent around the GO. (b) Time-resolved anisotropy for 460 nm excitation and 530 nm detection. The fluorescence was measured in water at pH 7 with the concentration adjusted to keep the OD below 0.1.

barely observed. The same trend was mirrored in the correlation functions (Figure 4b). The steady-state anisotropy in Figure 6a also decreased as the emission wavelength increased since the red-shifted emissions occurred further into the solvent's rotation.[27,33] If the wavelength-dependent emission was purely a result of the large distribution of size and functional groups in GO in the solution, the emission peak would have been constant with temperature, time, and anisotropy. The results presented prove that the wavelength-dependent emission in GO is only a result of the red-edge effect.

Insight into the Origin of the Giant Red-Edge Effect. If the solvation is much quicker than the fluorescence lifetime, like quantum dots or organic dyes, different excitation wavelengths relax to the same energy before emission and the red-edge effect is not present. Even if the solvation is slowed through high viscosity or low temperature in glasses, viscous polymers, proteins, and membranes, the peak emission wavelength is observed to shift only ~10 nm with changing the excitation wavelength, because the final solvated energy is reached quickly during the fluorescence lifetime.[33,38−40] The small red-edge shift in these cases is directly determined by the quick decay of the reported correlation functions, explaining why a small exponential peak shift is usually reported.[33,38−40] Contrary to these results, GO has a giant red-edge effect at room temperature in common solvents. Owing to the slow solvation dynamics, the fluorescence peak of GO red-shifted from 440 to 580 nm as the excitation wavelength changed from 350 to 500 nm (Figure 1e). The ratio of $\Delta\lambda_{emission}/\Delta\lambda_{excitation} \cong 1$ reflects the slow decay of the correlation function. The exponentially limited behavior of the red-edge effect reported previously was seen only in the limit of band edge excitation or high temperature, where solvent relaxation is complete during the fluorescence lifetime.

The TRF measurements in Figure 4 proved that the time-dependent emission energy $\omega(t)$ was the origin of the excitation wavelength dependent fluorescence. However, the TRF results cannot explain why $\omega(t)$ was so large and the measured correlation function had a longer lifetime than previously measured for fluorophores in organic solvents at room temperature. The strength of the time-dependent energy $U_{solv}(t)$, which induces the red-edge effect, is determined by μ_{fluo}, μ_{solv}, and $\Theta(t)$ (eq 4). The change in the excited-state dipole moment, μ_{fluo}, was estimated to be ~23 D by eq 7 using the fluorescence spectra in solvents of various polarities (Figure 7a and b) and assuming that the Onsager radius has a typical value of 5 Å.[27] This dipole moment is similar to many organic dyes with small red-edge effects.[27,48] The slope of the change in peak emission wavelength with change in excitation wavelength, $\Delta\lambda_{emission}/\Delta\lambda_{excitation} \cong 1$, was found to be independent of solvents with sufficient polarity > 0.2 and identical for the GO and the −OH-rich GO (Figure 7c). It should be noted that the Rayleigh filtering and the background subtraction can lead to some distortion of the excitation emission slope. These results ruled out the possibility of μ_{fluo} and μ_{solv} as the origin of the giant red-edge effect.

Since the magnitude of the solvent or the GO dipole moment was not responsible for the red-edge effect, the large shift in the time-dependent emission energy $\omega(t)$ must result from slow relaxation of the solvent and the excited-state dipole $\Theta(t)$. However, the measured solvent relaxation was ~650 ps, which is much greater than the solvation time of water, $\tau_{solv\text{-}water} \cong 1$ ps.[27,37] This means that an additional solvation process occurs, inducing the giant red-edge effect. This result also explains why the slope of the change in peak emission wavelength with changing excitation wavelength was independent of the polarity and solvation time of the organic solvent (Figure 7c), since an additional relaxation must be occurring at longer time scales than the solvent's solvation time.

The wavelength-dependent emission must be due to an additional interaction of the GO in the solvent. This can be investigated by looking at the time-resolved anisotropy (TRA) (Figure 6b), which measures the rotation of the fluorophore from its initial orientation at excitation. As the GO sheet rotates in the solvent, the polarization of the emission also rotates with respect to an initial value. The large size of the GO sheet means that physical rotation of the entire

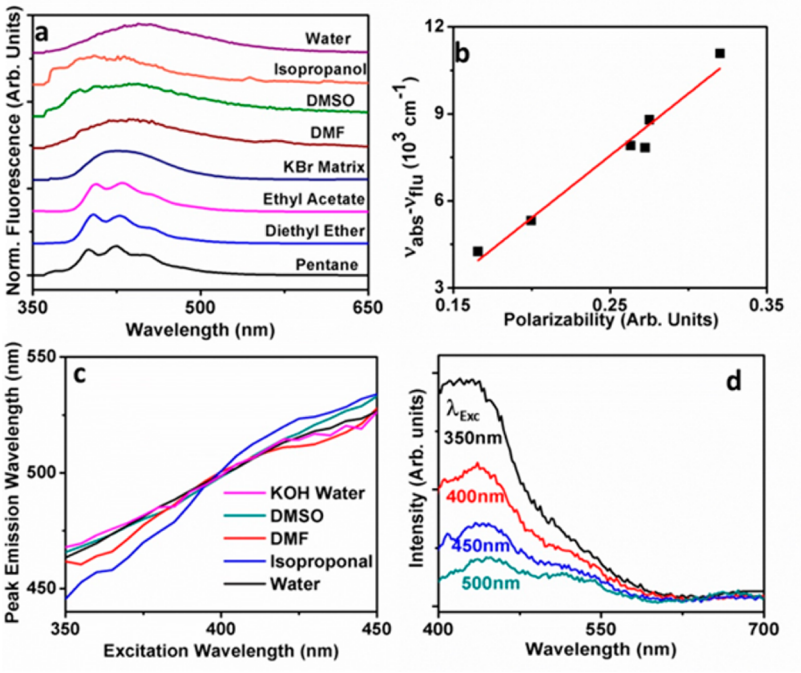

Figure 7. Effect of local environment on GO fluorescence. (a) Fluorescence of GO in solvents of increasing polarity under 350 nm excitation at neutral pH. (b) Peak emission wavelength plotted *versus* polarizability of the solvent. (c) Dependence of the change in emission wavelength with changing excitation wavelength for GO in several solvents and KOH treatment. (d) Fluorescence of single-layer GO immobilized on the glass under excitation with various excitation wavelengths for neutral pH in water.

emitting sheet will happen on a time scale of microseconds.[27] However, the TRA also showed a short time rotation of $\tau_{anis} = 670$ ps $\cong \tau_{solv} \gg \tau_{solv\text{-}water}$. This time scale was too short to represent rotation of the large 2D sheet, suggesting that the fluorescence dipole was reorienting in plane. To drive this rotation, the overall solvent relaxation must be occurring through additional interactions of the localized electron density of the fluorophore with the surrounding GO plane.

To gain insight into the source of the additional solvent interaction, single-layer GO was immobilized on glass. Fluorescence measurements were then performed on the immobilized single-layer GO in water. The single-layer GO exhibited a fluorescence emission that was independent of the excitation wavelength (Figure 7d). In addition, the excitation wavelength dependent fluorescence still occurred in the GO sheets that were soluble in the aqueous solution when the ionic strength of the solution was varied by changing the concentration of NaCl or $CaCl_2$. These results rule out the possibility that the interlayer interactions of GO in a solvent are the origin of the giant red-edge effect and instead suggest the GO sheet surrounding the localized electron density of the functional group/fluorophore undergoes an excited-state reorganization on the same time scale as the fluorescence lifetime. When the GO sheet is immobilized or in a nonpolar solvent, the local interaction is reduced since the possible local reorganization is negligible, and no red edge effect is seen. This is consistent with the previously reported luminescence maps for immobilized and solvated GO.[49]

This possible explanation is consistent with the small red-edge effect measured for traditional organic dyes in a protein or molecular matrix where the local solvation environment is not determined by the solvent, but the local environment of the fluorophore.[28,38] However, unlike a dye in a rigid matrix, no external matrix is needed to induce a giant red-edge shift in GO. Instead, the local reorganization of GO sheets slows the solvation dynamics to a scale where the red-edge effect exists strongly in water at room temperature. The reorganization exists regardless of the strength or the polarizability of the solvent, although it is only in a polar solvent that the solvation time becomes comparable to the fluorescence lifetime, allowing the giant red-edge effect. The suggested local reorganization mechanism is thus consistent with the reports of the small change in emission energy and TRA seen on a ~1 ps time scale for multilayer GO in air and the small excitation wavelength dependent fluorescence of GO-coated paper.[35,50]

It is noted that there exist a large number of different sized π-conjugated fragments and functional groups in the GO sheets. If the excitation wavelength dependent emission was due to the continual excitation of different sized conjugated π fragments in the GO, this phenomenon would have not changed in any of the following three cases: (i) when the polar solution containing the GO sheets was heated to 80 °C; (ii) when

the GO sheets were suspended in a nonpolar solvent; and (iii) when a GO sheet was fixed on a rigid solid-state state. In fact, our experiments have shown that the excitation wavelength dependent emission disappeared in all three cases (Figures 1, S1, and 7). Keeping in mind that each of these experiments changed only the dynamics of the solvent relaxation and did not change the structure and the chemical properties of the GO or modify the possible subset of π-conjugated fragments that could fluoresce, we can rule out the possibility that excitation wavelength dependent emission was originated from the continual excitation of different sized conjugated π fragments in the GO.

In particular, the measurements of GO fluorescence in a nonpolar solvent have shown that the distribution of π-conjugated fragments only broadened the molecular transitions (Figure 1). This led to a slight tail of the emission, but the effect was small compared to the fluorescence in the polar solvent. This was because in a polar solvent, in addition to the distribution-based broadening like in a nonpolar solvent, the excitation energy was redistributed over a large energy range due to the giant red-edge effect, extending the solvation time scale to that of the fluorescence. Since the molecular transitions re-emit over a changing final energy, the initially narrower absorption peak can lead to a large range of emission wavelengths, which will depend on the initial excitation energy and in which relaxed energy states can be reached before fluorescence occurs. The dynamic nature of the excitation wavelength-dependent emission and the spectral broadening in GO explains not only the dependence on environment, as shown in this study, but also the remarkable consistency of the peak emission wavelength shift *versus* excitation wavelength that can be found in the literature for GO and GO nanodots, even if the chemical treatment and initial emission spectrum may vary.[5−26]

CONCLUSIONS

The fluorescence of GO is a combination of an excited-state protonation of the −COOH group and an excitation wavelength dependent fluorescence from the polar groups such as the −OH moiety in the GO sheets. The two independent components are responsible for the broad fluorescent emission of GO at low pH. At high pH or after chemical reduction of GO in the KOH solution, the polar groups such as the −OH moiety dominate the fluorescence, which depends on the excitation wavelength. Time-resolved fluorescence measurements of GO suggest that local reorganization of GO sheets slows the solvation dynamics of photoexcited electrons in a polar solvent. As a result, the solvent relaxation time becomes comparable to the fluorescence lifetime, creating the time-dependent fluorescence emission energy, allowing the giant red-edge effect. The giant red-edge effect is responsible for the strong dependence of the fluorescence peak position upon the wavelength of the excitation source. When the temperature increases, the solvation dynamics becomes faster and mitigate the giant red-edge effect. The giant red-edge effect of GO disappears in a nonpolar solvent, leading to a fluorescence peak independent of the excitation wavelength. The solvation process is also responsible for the broad bandwidth of GO's fluorescence in a polar solvent. In contrast, GO shows a narrow fluorescence peak in a nonpolar solvent.

Application of the giant red-edge effect has been nonexistent when compared to the other emergent phenomena in the graphene family of materials. This study has discovered the underlying mechanism of strong excitation wavelength dependent fluorescence in GO, which can open many exciting opportunities because the fluorescence wavelength can be changed *in situ* by simply changing the excitation wavelength. Further, the red-edge effect mechanism can be extended to carbon quantum dots, where the same excitation wavelength dependent emission and spectral tuning is present identical to that in GO sheets.[5−9,13,17,20,22,25,26,50] The red-edge effect could therefore allow the small carbon quantum dots to be used simultaneously as a fluorescence tag by the emission wavelength and a probe of the polarizability of the local environment by the extent of the red-edge effect.[28−30,38] The broad absorption and the emission of the giant red-edge effect is expected to have implications in biological sensing, tunable full spectrum fluorescent light sources, optoelectronics and solar energy harvesting, or new areas of photoluminescence research.

METHODS

Synthesis of Graphene Oxide. Chemical exfoliation of graphite was used to achieve the GO sheet according to the well-documented Hummers method.[51] The GO sheets were immersed into the KOH aqueous solution, leading to hydroxyl groups on the carbon skeleton. To obtain the carboxyl-rich GO, the GO sheets were treated in the HNO_3 solution. The detailed procedures can be found in our previous paper.[15] Finally, the KOH- and HNO_3-treated GO sheets were dried overnight in a vacuum oven at room temperature. The KOH- and HNO_3-treated GO sheets were added into DI water to obtain a concentration of 100 μg/mL GO for further use.

To immobilize the graphene oxide sheets on the glass substrate, the loose and brown GO powder was suspended in water (0.5 mg/mL). The fresh glass substrate was then immersed into the aqueous GO suspension, followed by slow pulling (2 mm/s). This resulted in the attachment of a single-layer GO sheet on the glass. The GO-immobilized substrates were then dried in air for use.

Characterization and Optics. The UV−visible absorption properties were measured with a Shimadzu UV-2550 spectrometer (Shimadzu Co., Kyoto, Japan). The KBr pellet containing the GO sample was used to acquire the Fourier-transform infrared (FT-IR) spectra under the transmission mode with a Nicolet

6700 spectrometer (Thermo Scientific, Waltham, MA, USA). The functional groups in the GO samples were also characterized with X-ray photoelectron spectroscopy (XPS) using a PHI 5000 Versa Probe system (Physical Electronics, MN, USA). The XPS spectra were calibrated with reference to the C 1s peak of the sp^2 carbon atoms at 284.6 eV.

Fluorescence measurements were recorded with a double-monochromated Horiba Jobin Yvon Fluorolog-3 spectrofluorometer. The pH of GO solution was 5, 7, and 3 for the pristine and −OH- and −COOH-functionalized graphene oxide spectra shown in Figure 2. The pH was neutral in all other measurements unless otherwise noted. Absorption was kept below 0.1 OD for all solutions to prevent inner filter effects. All samples were stirred and kept at 20 °C unless otherwise noted. Raman scattering and instrument response were corrected. Time-resolved spectra were captured using time-correlated single photon counting (TCSPC) with a pulsed LED light source at 460 or 370 nm. Anisotropy was defined as $r = (I_{\parallel} - I_{\perp})/(I_{\parallel} + 2I_{\perp})$, where $I_{\parallel}$ and $I_{\perp}$ refer to the light parallel and perpendicular to the incident polarization. The center of mass was calculated as $\nu_{cg} = \int \nu^* f(\nu)\, d\nu / \int f(\nu)\, d\nu$, where $f(\nu)$ is the fluorescence spectrum.[27] The TRES spectra were normalized in the manner described previously.[27] The full TRES spectra are shown in Figure S5 for each temperature. The full 2D excitation emission plots from which the center of emission was calculated are shown in Figure S7 for temperature and Figure S8 for the various solvents. Polarizability was defined as $f(\varepsilon,n) = ((\varepsilon - 1)/(2\varepsilon + 1)) + ((n^2 - 1)/(2n^2 + 1))$ where ε is the dielectric constant and n is the refractive index.

Conflict of Interest: The authors declare no competing financial interest.

Acknowledgment. This work was supported by the National Science Foundation (CBET-1336205) and NSF Graduate Research Fellowship (1102689). The resource and facilities used were partially supported by NSF (EPS 1003907), the West Virginia University Research Corporation, and the West Virginia EPSCoR Office. The use of WVU shared facility is acknowledged.

Supporting Information Available: Figures S1−S8 and Table S1. This material is available free of charge *via* the Internet at http://pubs.acs.org.

REFERENCES AND NOTES

1. Geim, A. K; Novoselov, K. S. The Rise of Graphene. *Nat. Mater.* **2007**, *6*, 183–191.
2. Novoselov, K. S.; Fal, V. I.; Colombo, L.; Gellert, P. R.; Schwab, M. G.; Kim, K. A Roadmap for Graphene. *Nature* **2012**, *490*, 192–200.
3. Bonaccorso, F.; Sun, Z.; Hasan, T.; Ferrari, A. C. Graphene Photonics and Optoelectronics. *Nat. Photonics* **2010**, *4*, 611–622.
4. Xiang, Q.; Yu, J.; Jaroniec, M. Graphene-Based Semiconductor Photocatalysts. *Chem. Soc. Rev.* **2012**, *41*, 782–796.
5. Pan, D.; Zhang, J.; Li, Z.; Wu, M. Hydrothermal Route for Cutting Graphene Sheets into Blue-Luminescent Graphene Quantum Dots. *Adv. Mater.* **2010**, *22*, 734–738.
6. Pan, D.; Guo, L.; Zhang, J.; Xi, C.; Xue, Q.; Huang, H.; Li, J.; Zhang, Z.; Yu, W.; Chen, Z.; *et al.* Cutting sp^2 Clusters in Graphene Sheets into Colloidal Graphene Quantum Dots with Strong Green Fluorescence. *J. Mater. Chem.* **2012**, *22*, 3314–3318.
7. Zhu, S.; Tang, S.; Zhang, J.; Yang, B. Control the Size and Surface Chemistry of Graphene for the Rising Fluorescent Materials. *Chem. Commun.* **2012**, *48*, 4527–4539.
8. Mueller, M. L.; Yan, X.; McGuire, J.; Li, L. Triplet States and Electronic Relaxation in Photoexcited Graphene Quantum Dots. *Nano Lett.* **2010**, *10*, 2679–2682.
9. Liu, R.; Wu, D.; Feng, X.; Mullen, K. Bottom-Up Fabrication of Photoluminescent Graphene Quantum Dots with Uniform Morphology. *J. Am. Chem. Soc.* **2011**, *133*, 15221–15223.
10. Loh, K. P.; Bao, Q.; Eda, G.; Chhowalla, M. Graphene Oxide as a Chemically Tunable Platform for Optical Applications. *Nat. Chem.* **2010**, *2*, 1015–1024.
11. Eda, G.; Lin, Y. Y.; Mattevi, C.; Yamaguchi, H.; Chen, H. A.; Chen, I.; Chen, C. W.; Chhowalla, M. Blue Photoluminescence from Chemically Derived Graphene Oxide. *Adv. Mater.* **2010**, *22*, 505–509.
12. Mei, Q.; Zhang, K.; Guan, G.; Liu, B.; Wang, S.; Zhang, Z. Highly Efficient Photoluminescent Graphene Oxide with Tunable Surface Properties. *Chem. Commun.* **2010**, *46*, 7319–7321.
13. Shen, J.; Zhu, Y.; Yang, X.; Li, C. Graphene Quantum Dots: Emergent Nanolights for Bioimaging, Sensors, Catalysis and Photovoltaic Devices. *Chem. Commun.* **2012**, *48*, 3686–3699.
14. Chien, C. T.; Li, S. S.; Lai, W. J.; Yeh, Y. C.; Chen, H. A.; Chen, I.; Chen, L. C.; Chen, K. H.; Nemoto, T.; Isoda, S.; *et al.* Tunable Photoluminescence from Graphene Oxide. *Angew. Chem., Int. Ed.* **2012**, *51*, 6662–6666.
15. Li, M.; Cushing, S. K.; Zhou, X.; Guo, S.; Wu, N. Q. Fingerprinting Photoluminescence of Functional Groups in Graphene Oxide. *J. Mater. Chem.* **2012**, *22*, 23374–23379.
16. Galande, C.; Mohite, A. D.; Naumov, A. V.; Gao, W.; Ci, L.; Ajayan, A.; Gao, H.; Srivastava, A.; Weisman, R. B.; Ajayan, P. M. Quasi-Molecular Fluorescence from Graphene Oxide. *Sci. Rep.* **2011**, *1*, 85.
17. Li, Y.; Zhao, Y.; Cheng, H.; Hu, Y.; Shi, G.; Dai, L.; Qu, L. Nitrogen-Doped Graphene Quantum Dots with Oxygen-Rich Functional Groups. *J. Am. Chem. Soc.* **2012**, *134*, 15–18.
18. Zhang, X. F.; Shao, X.; Liu, S. Dual Fluorescence of Graphene Oxide: A Time-Resolved Study. *J. Phys. Chem. A* **2012**, *116*, 7308–7313.
19. Wang, D.; Wang, L.; Dong, X.; Shi, Z.; Jin, J. Chemically Tailoring Graphene Oxides into Fluorescent Nanosheets for Fe^{3+} Ion Detection. *Carbon* **2012**, *50*, 2147–2154.
20. Baker, S. N.; Baker, G. A. Luminescent Carbon Nanodots: Emergent Nanolights. *Angew. Chem., Int. Ed.* **2010**, *49*, 6726–6744.
21. Gokus, T.; Nair, R. R.; Bonetti, A.; Bohmler, M.; Lombardo, A.; Novoselov, K. S.; Geim, A. K.; Ferrari, A. C.; Hartschuh, A. Making Graphene Luminescent by Oxygen Plasma Treatment. *ACS Nano* **2009**, *3*, 3963–3968.
22. Shen, J.; Zhu, Y.; Yang, X.; Zong, J.; Zhang, J.; Li, C. One-Pot Hydrothermal Synthesis of Graphene Quantum Dots Surface-Passivated by Polyethylene Glycol and Their Photoelectric Conversion under Near-Infrared Light. *New J. Chem.* **2012**, *36*, 97–101.
23. Ferrari, A. C.; Meyer, J. C.; Scardaci, V.; Casiraghi, C.; Lazzeri, M.; Mauri, F.; Piscanec, S.; Jiang, D.; Novoselov, K. S.; Roth, S.; Geim, A. K. Raman Spectrum of Graphene and Graphene Layers. *Phys. Rev. Lett.* **2006**, *97*, 187401.
24. Yang, S.; Zeng, H.; Zhao, H.; Zhang, H.; Cai, W. Luminescent Hollow Carbon Shells and Fullerene-Like Carbon Spheres Produced by Laser Ablation with Toluene. *J. Mater. Chem.* **2011**, *21*, 4432–4436.
25. Sun, Y. P.; Zhou, B.; Lin, Y.; Wang, W.; Fernando, K. S.; Pathak, P.; Meziani, M. J.; Haruff, B. A.; Wang, X.; Wang, H.; *et al.* Quantum-Sized Carbon Dots for Bright and Colorful Photoluminescence. *J. Am. Chem. Soc.* **2006**, *128*, 7756–7757.
26. Bourlinos, A. B.; Zbořil, R.; Petr, J.; Bakandritsos, A.; Krysmann, M.; Giannelis, E. P. Luminescent Surface Quaternized Carbon Dots. *Chem. Mater.* **2011**, *24*, 6–8.
27. Lakowicz, J. R. In *Principles of Fluorescence Spectroscopy*; Springer Academic: New York, 2006.
28. Haldar, S.; Chaudhuri, A.; Chattopadhyay, A. Organization and Dynamics of Membrane Probes and Proteins Utilizing the Red Edge Excitation Shift. *J. Phys. Chem. B* **2011**, *115*, 5693–5706.
29. Demchenko, P.; Sytnik, I. Solvent Reorganizational Red-Edge Effect in Intramolecular Electron Transfer. *Proc. Natl. Acad. Sci. U.S.A.* **1991**, *88*, 9311–9344.
30. Haldar, S.; Chattopadhyay, A. Dipolar Relaxation within the Protein Matrix of the Green Fluorescent Protein: A Red Edge Excitation Shift Study. *J. Phys. Chem. B* **2007**, *111*, 14436–14439.
31. Hu, Z.; Margulis, C. J. Room-Temperature Ionic Liquids: Slow Dynamics, Viscosity, and the Red Edge Effect. *Acc. Chem. Res.* **2007**, *40*, 1097–1105.

32. Xiao, L.; Xu, Y.; Yan, M.; Galipeau, D.; Peng, X.; Yan, X. Excitation-Dependent Fluorescence of Triphenylamine-Substituted Tridentate Pyridyl Ruthenium Complexes. *J. Phys. Chem. A* **2010**, *114*, 9090–9097.
33. Khara, D. C.; Samanta, A. Solvation Dynamics and Red-Edge Effect of Two Electrically Charged Solutes in an Imidazolium Ionic Liquid. *Indian J. Chem.* **2010**, *49*, 714–720.
34. Kaniyankandy, S.; Achary, S. N.; Rawalekar, S.; Ghosh, H. N. Ultrafast Relaxation Dynamics in Graphene Oxide: Evidence of Electron Trapping. *J. Phys. Chem. C* **2011**, *115*, 19110–19116.
35. Exarhos, A. L.; Turk, M. E.; Kikkawa, J. M. Ultrafast Spectral Migration of Photoluminescence in Graphene Oxide. *Nano Lett.* **2013**, *13*, 344–349.
36. Kasha, M. Characterization of Electronic Transitions in Complex Molecules. *Discuss. Faraday Soc.* **1950**, *9*, 14–19.
37. Reynolds, L.; Gardecki, J. A.; Frankland, S. J.; Horng, M. L.; Maroncelli, M. Dipole Solvation in Nondipolar Solvents: Experimental Studies of Reorganization Energies. *J. Phys. Chem.* **1996**, *100*, 10337–10354.
38. Demchenko, A. P. The Red-Edge Effects: 30 Years of Exploration. *Luminescence* **2002**, *17*, 19–42.
39. Józefowicz, M.; Heldt, J. R. Excitation-Wavelength Dependent Fluorescence of Ethyl 5-(4-aminophenyl)-3-amino-2,4-dicyanobenzoate. *J. Fluoresc.* **2011**, *21*, 239–245.
40. Samanta, A. Dynamic Stokes Shift and Excitation Wavelength Dependent Fluorescence of Dipolar Molecules in Room Temperature Ionic Liquids. *J. Phys. Chem. B* **2006**, *110*, 13704–13716.
41. Mathkar, A.; Tozier, D.; Cox, P.; Ong, P.; Galande, C.; Balakrishnan, K.; Reddy, A. L. M.; Ajayan, P. M. Controlled, Stepwise Reduction and Band Gap Manipulation of Graphene Oxide. *J. Phys. Chem. Lett.* **2012**, *3*, 986–991.
42. Zhao, F.; Liu, J.; Huang, X.; Zou, X.; Lu, G.; Sun, P.; Wu, S.; Ai, W.; Yi, M.; Qi, X.; *et al*. Chemoselective Photodeoxidization of Graphene Oxide Using Sterically Hindered Amines as Catalyst: Synthesis and Applications. *ACS Nano* **2012**, *6*, 3027–3033.
43. Kravets, V. G.; Grigorenko, A. N.; Nair, R. R.; Blake, P.; Anissimova, S.; Novoselov, K. S.; Geim, A. K. Spectroscopic Ellipsometry of Graphene and an Exciton-Shifted Van Hove Peak in Absorption. *Phys. Rev. B* **2010**, *81*, 155413.
44. Balog, R.; Jørgensen, B.; Nilsson, L.; Andersen, M.; Rienks, E.; Bianchi, M.; Fanetti, M.; Lægsgaard, E.; Baraldi, A.; Lizzit, S.; *et al*. Bandgap Opening in Graphene Induced by Patterned Hydrogen Adsorption. *Nat. Mater.* **2010**, *9*, 315–319.
45. Van der Zwan, G.; Hynes, J. T. Time-Dependent Fluorescence Solvent Shifts, Dielectric Friction, and Nonequilibrium Solvation in Polar Solvents. *J. Phys. Chem.* **1985**, *89*, 4181–4188.
46. Simon, J. D. Time-Resolved Studies of Solvation in Polar Media. *Acc. Chem. Res.* **1988**, *21*, 128–134.
47. Brady, J.; Carr, P. An Analysis of Dielectric Models of Solvatochromism. *J. Phys. Chem.* **1985**, *89*, 5759–5766.
48. Hutterer, R.; Parusel, A. B. J.; Hof, M. Solvent Relaxation of Prodan and Patman: A Useful Tool for the Determination of Polarity and Rigidity Changes in Membranes. *J. Fluoresc.* **1998**, *8*, 389–393.
49. Luo, Z.; Vora, P. M.; Mele, E. J.; Johnson, A. T. C.; Kikkawa, J. M. Photoluminescence and Band Gap Modulation in Graphene Oxide. *Appl. Phys. Lett.* **2009**, *94*, 11909.
50. Qu, S.; Wang, X.; Lu, Q.; Liu, X.; Wang, L. A Biocompatible Fluorescent Ink Based on Water-Soluble Luminescent Carbon Nanodots. *Angew. Chem., Int. Ed.* **2012**, *51*, 12215–12218.
51. Hummers, W. S.; Offeman, R. E. Preparation of Graphitic Oxide. *J. Am. Chem. Soc.* **1958**, *80*, 1339–1339.